

REVIEW ARTICLE

The measurement and interpretation of superallowed $0^+ \rightarrow 0^+$ nuclear β decay

J C Hardy and I S Towner

Cyclotron Institute, Texas A&M University, College Station, TX 77843-3366, U.S.A.

E-mail: hardy@comp.tamu.edu, towner@comp.tamu.edu

Abstract. Measurements of the decay strength of superallowed $0^+ \rightarrow 0^+$ nuclear β transitions shed light on the fundamental properties of weak interactions. Because of their impact, such measurements were first reported 60 years ago in the early 1950s and have continued unabated ever since, always taking advantage of improvements in experimental techniques to achieve ever higher precision. The results helped first to shape the Electroweak Standard Model but more recently have evolved into sensitively testing that model's predictions. Today they provide the most demanding test of vector-current conservation and of the unitarity of the Cabibbo-Kobayashi-Maskawa matrix. Here, we review the experimental and theoretical methods that have been, and are being, used to characterize superallowed $0^+ \rightarrow 0^+$ β transitions and to extract fundamentally important parameters from their analysis.

1. Introduction

In 1953, Sherr and Gerhart published a paper [1] on “Experimental evidence for the Fermi interaction in the β decay of ^{14}O and ^{10}C .” It was less than five years since Sherr had first discovered these two nuclei [2], yet already the two authors were using the decays to probe for the first time the fundamental nature of β decay. They were able to identify superallowed transitions in both decays – they called them “allowed favoured transitions” – and recognized that the Fermi theory of β decay predicted that the comparative half-lives, or ft values, for the two transitions should be the same, a prediction they could test. The ft value for a transition depends on the energy released by the transition as well as its branching ratio and the half-life of the initial state. Using degraders to determine the energy of the emitted positrons, a NaI(Tl) scintillation spectrometer to establish the branching ratios and Geiger counters to measure the half lives, Sherr and Gerhard were able to conclude that the two ft values were indeed the same, albeit with large error bars: They obtained 3300 ± 750 s for the superallowed ft value of ^{14}O and 5900 ± 2400 s for that of ^{10}C .

By 1960, when Bardin *et al.* reported a much improved result for ^{14}O [3], experimental techniques had advanced considerably. The decay energy was no longer dependent on positron range measurements, but rather on measured Q values for

the reactions $^{12}\text{C}(^3\text{He},n)^{14}\text{O}$ and $^{12}\text{C}(^3\text{He},p)^{14}\text{N}^*$, which populated the superallowed transition's parent and daughter states, respectively, from a common target. Also, the branching ratio could be corrected for the weak non-superallowed β branch to the ground state of ^{14}N , which had by then been measured with the help of a magnetic lens spectrometer [4]. They reported an ft value of 3060 ± 13 s, which for its time is a remarkably precise result and stands only 1.4 standard deviations away from the currently accepted value of 3042.3 ± 2.7 s.

The precision obtained by Bardin *et al.* was sufficient for them to compare the vector coupling constant G_V , derived from their ft -value, with G_F , the weak-interaction constant derived from the purely leptonic decay of the muon. The Conserved Vector Current (CVC) hypothesis had been proposed by Feynman and Gell-Mann two years earlier [5] but the role of strangeness was not yet understood, so the authors expected that G_V should equal G_F . Although their measurement actually showed a small difference between the two, the authors noted that radiative and Coulomb corrections could account for the discrepancy and concluded that it was too soon to tell if this constituted a failure of the universality hypothesis.

The discrepancy persisted, however, and was joined by other discrepancies observed between weak decays that changed strangeness S and those that did not, the most glaring example being the decays of the K^+ ($S=1$) and the π^+ ($S=0$) mesons to the same final state, $\mu^+ + \nu$. All these apparent conflicts with vector-current universality were resolved by Cabibbo in 1963 [6] when he recognized that the universality of the weak interaction was manifest only if one considered the total strength of both the strangeness non-changing and the strangeness changing decays. In modern terminology we would say that he was the first to realize that there is mixing between the first two generations of quarks, and to express that mixing in terms of a unitary rotation.

As it turned out, that was only part of the story. A year after Cabibbo introduced his rotation angle, another symmetry – that of CP – was observed to be violated in the weak decay of the long-lived neutral kaon. This result, which remained a puzzle for nearly a decade, ultimately led Kobayashi and Maskawa [7] in 1973 to postulate the existence of a third generation of quarks – subsequently confirmed by experiment – and to replace Cabibbo's single rotation angle θ_C , which was in effect a 2×2 rotation matrix, by the now familiar 3×3 unitary rotation matrix referred to as the Cabibbo-Kobayashi-Maskawa, or CKM, matrix. It became one of the pillars of the Standard Model.

In the conclusion to his 1963 paper, Cabibbo remarked that G_V should no longer be expected to be equal to G_F but rather to $G_F \cos \theta_C$. However, he noted that although this change was “in the right direction to eliminate the discrepancy between ^{14}O and muon lifetimes,” in fact the correction was “too large, leaving about 2% to be explained” [6]. That observation was enough to stimulate a great deal of activity in superallowed β decay during the decade between Cabibbo's insight and that of Kobayashi and Maskawa. By 1973, the number of well-measured superallowed transitions had grown from one to seven; the 2% discrepancy was being explained in terms of radiative corrections and

charge-dependent nuclear corrections [8]; and plausible values for the Cabibbo angle had been extracted from the results. Once the CKM matrix took center stage though, it was not long before the focus of superallowed β decay had shifted to a determination of the upper left element of the CKM matrix, V_{ud} , the value of which is in fact closely related to $\cos \theta_C$.

Today, 40 years on, although the Standard Model is by now well established, the limits of its applicability are still being probed aggressively. One such experimental probe is to test the unitarity of the CKM matrix. Although the Standard Model does not prescribe values for the nine elements of the matrix – they must all be determined from experiment – it does require the matrix itself to be unitary. Superallowed β decay is currently the source of the most precise value for V_{ud} [9, 10], which is the largest element in the matrix, and is therefore a crucial contributor to the most sensitive available test of CKM unitarity: the sum of squares of the three top-row elements [11]. The current value for that unitarity sum is 1.00008 ± 0.00056 [12], a remarkably precise result that agrees with unitarity and significantly limits the scope for new physics beyond the Standard Model. However, even this precision, $\pm 0.06\%$, will likely be improved before long by upgraded measurements of superallowed transitions, which are already underway.

In what follows we review particularly the experimental methods that have been, and are being, used to characterize superallowed $0^+ \rightarrow 0^+$ β transitions. Although these are all nuclear-physics measurements, the extraordinary demands for precision in the Standard-Model test have motivated the development of highly refined techniques not commonly employed in other nuclear-physics applications. In addition, since theory also plays a vital role in the extraction of V_{ud} , we also outline the methods used for calculating the small radiative and isospin-symmetry-breaking corrections that must be applied to the experimental data.

2. Experiments, past and present

Since the axial current cannot contribute to transitions between spin-0 states, superallowed $0^+ \rightarrow 0^+$ β decay between $T=1$ analogue states depends uniquely on the vector part of the weak interaction. As already noted, the CVC principle indicates that the experimental ft value for such a transition should be related to the vector coupling constant, G_V , which must be common to all nuclear vector transitions. In turn, G_V itself is related to the fundamental weak-interaction coupling constant, G_F , via the relation

$$G_V = G_F V_{ud}, \tag{1}$$

where $G_F/(\hbar c)^3 = (1.1663787 \pm 0.0000006) \times 10^{-5} \text{ GeV}^{-2}$, as obtained from the measured muon lifetime [10]

In practice, the expression for ft includes several small correction terms. It is convenient to combine some of these terms with the ft value and define a “corrected” $\mathcal{F}t$ value. Thus, we write [9]

$$\mathcal{F}t \equiv ft(1 + \delta'_R)(1 + \delta_{NS} - \delta_C) = \frac{K}{2G_V^2(1 + \Delta_R^V)}, \tag{2}$$

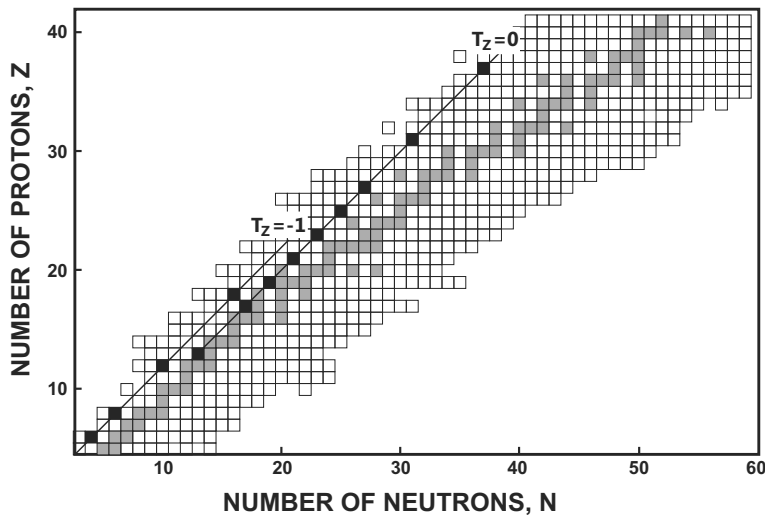


Figure 1. Partial chart of nuclides showing parents of the precisely measured superallowed transitions as solid black squares. The stable nuclei appear as grey squares. The two labeled diagonal lines mark the loci of the $T_Z = -1$ and $T_Z = 0$ parents. From left to right, the former are ^{10}C , ^{14}O , ^{22}Mg and ^{34}Ar ; and the latter are ^{26m}Al , ^{34}Cl , ^{38m}K , ^{42}Sc , ^{46}V , ^{50}Mn , ^{54}Co , ^{62}Ga and ^{74}Rb .

where $K/(\hbar c)^6 = 2\pi^3 \hbar \ln 2 / (m_e c^2)^5 = 8120.2787(11) \times 10^{-10} \text{ GeV}^{-4}\text{s}$, δ_C is the isospin-symmetry-breaking correction, and Δ_R^V is the transition-independent part of the radiative correction. The terms δ'_R and δ_{NS} comprise the transition-dependent part of the radiative correction, the former being a function only of the electron's energy and the Z of the daughter nucleus, while the latter, like δ_C , depends in its evaluation on the details of the nuclear structure of the parent and daughter states. All these correction terms are of order 1% or less, with uncertainties at least an order of magnitude smaller than that, so equation (2) provides an experimental method for determining G_V – and thus V_{ud} – to better than a part in a thousand.

Experimentally, the ft value that characterizes a superallowed transition – or any β transition for that matter – is determined from three measured quantities: the total transition energy, Q_{EC} , the half-life, $t_{1/2}$, of the parent state, and the branching ratio, R , for the particular transition of interest. The Q_{EC} -value is required to determine the phase-space integral, f , while the half-life and branching ratio combine to yield the partial half-life, t . Since the ft value incorporates three experimental quantities, each one of those quantities must be measured to substantially better than 0.1% precision in order to achieve that precision on the combination. This is particularly true for Q_{EC} since it enters to the fifth power in the calculation of f .

To date, the ft values for ten $0^+ \rightarrow 0^+$ transitions – with parents ^{14}O , ^{26m}Al , ^{34}Cl , ^{38m}K , ^{42}Sc , ^{46}V , ^{50}Mn , ^{54}Co , ^{62}Ga and ^{74}Rb – are known to 0.1% relative precision or better; and three more – ^{10}C , ^{22}Mg and ^{34}Ar – are known to $<0.3\%$. The 13 cases are shown on the chart of nuclides in Fig. 1. How has this level of precision been achieved in all these cases for the combination of three experimental quantities? In answering this question in the following sections, we frequently reference examples of

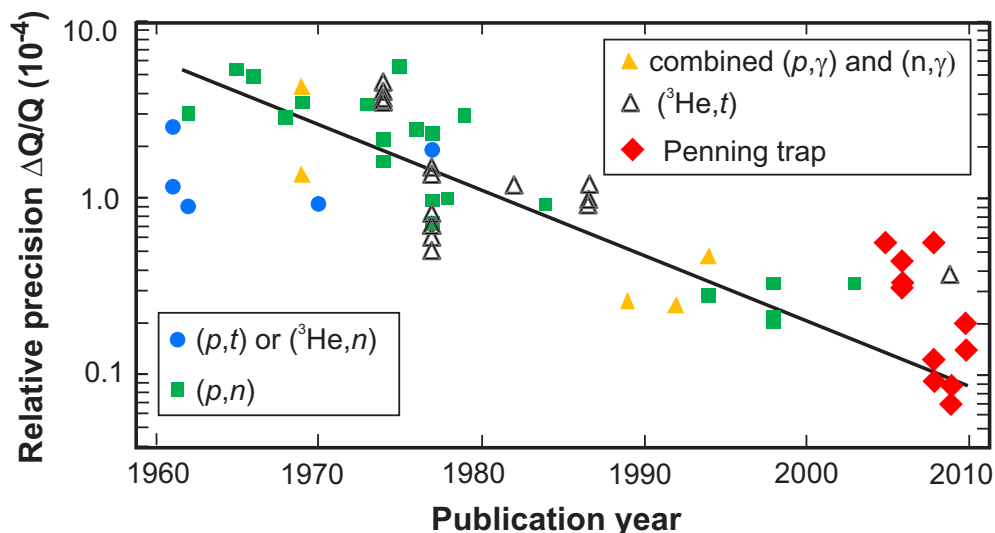


Figure 2. The relative precision, $\Delta Q/Q$, for Q_{EC} -value measurements of superallowed transitions is plotted against their publication date, where Q is the measured Q_{EC} value and ΔQ is its quoted uncertainty. The data encompass the superallowed transitions from ^{10}C , ^{14}O , ^{26m}Al , ^{34}Cl , ^{38m}K , ^{42}Sc , ^{46}V , ^{50}Mn and ^{54}Co , and are taken from a series of survey articles [9, 13, 14, 15] plus two more-recent publications [16, 17]. Each point is identified by the experimental method used in the corresponding measurement. The line simply illustrates the decreasing trend. (Adapted from ref. [18].)

various measurement techniques. A complete referenced list of *all* measurements that currently contribute to world data for superallowed $0^+ \rightarrow 0^+$ decays appears in the 2009 survey by Hardy and Towner [9].

2.1. Q_{EC} -value measurements

Already in 1960, Barden *et al.* [3] appreciated that a determination of the end-point energy from a measured β spectrum, even if that spectrum were obtained with a magnetic spectrometer, could not possibly match the precision possible with a nuclear reaction. From that time on, until the advent of on-line Penning traps less than a decade ago, nuclear reactions were the only method used to determine precise Q_{EC} values. The favoured ones were (p, n) and $(^3\text{He}, t)$ reactions on the β -decay daughter nuclei, which are stable for all $0^+ \rightarrow 0^+$ superallowed decays that have been studied until recently. Since these reactions connect the same nuclei as the corresponding β decay, their Q values are directly related to the β -decay Q_{EC} value.

The relative precision, $\Delta Q/Q$, obtained for various measurements and techniques is plotted in Fig. 2 as a function of publication date, starting in 1960. Evidently the relative precision improved steadily over the years, from $\sim 5 \times 10^{-4}$ in the early 1960s to $\sim 3 \times 10^{-5}$ by 1990, but at that point a limit seemed to have been reached: for the next fifteen years there were no further improvements in Q_{EC} -value precision, not even with the appearance of the first few Penning-trap measurements. However, the figure shows that in the space of only a few years after their first contribution, Penning traps had

improved the relative precision for measured Q_{EC} values by a factor of 5, to as low as $\sim 7 \times 10^{-6}$. To put this last number into perspective, it applies to the decay of ^{38m}K and corresponds to an uncertainty of ± 40 eV on a total Q_{EC} value of 6044.22 keV [16].

Although Penning traps are now outstripping nuclear reactions in the precision of their Q_{EC} -value results, for each transition it is the average of all measurements with uncertainties within a factor of ten of the best measurement that is used in the determination of V_{ud} . Many reaction measurements therefore still make significant contributions to the world averages for Q_{EC} values. We will describe several examples of important reaction measurements before doing the same for Penning-trap measurements.

2.1.1. The (p,n) reaction It can easily be seen in Fig. 2 that before 2005 the dominant choice for making Q_{EC} -value measurements of $0^+ \rightarrow 0^+$ transitions was the (p,n) reaction. There are a total of 21 such cases documented in the figure, with all but one – the first – being threshold measurements. Between 1962 and 1976, all but two of the measurements were made by Freeman and her collaborators using the 12 MeV Tandem accelerator at Harwell in England (e.g. [19, 20]). From 1977 on, all but two were made by Barker *et al.* using the folded Tandem accelerator AURA2 at the University of Auckland in New Zealand (e.g. [21, 22]).

The Freeman measurements and the early Barker measurements all used the same general approach: For a superallowed decay $P \rightarrow D$ they bombarded a thin target of the daughter material D with a proton beam for a well-determined time, and then interrupted the beam while they determined the amount of the parent P that had been produced by recording the characteristic activity of P, usually its emitted positrons. This beam on-off cycle was repeated until sufficient statistics had been accumulated. Then the process was repeated at a succession of different beam energies until a threshold curve for the production of P had been obtained. They calibrated the proton beam energy near threshold by scattering the beam at 90° from a thin gold foil into a broad-range magnetic spectrograph, where it was compared with a known α -particle group from the decay of a standard source such as ^{212}Po . This, of course, meant that the accuracy of their threshold energy – and the resultant Q_{EC} value – relied upon the accuracy of the α -particle energy as it was known at the time but, by clearly indicating the α energy they used, they ensured that their result could be upgraded in future whenever that calibration energy was improved.

Barker's group refined this technique by passing the primary proton beam through an Enge split-pole magnetic spectrograph, which was set at 0° . The beam path and width were constrained by a set of slots and apertures, resulting in an energy profile with FWHM (full width half maximum) of 50-100 ppm (parts per million) at the focal plane of the spectrograph [22]. It was this prepared beam that bombarded the target, which was located 50 cm beyond the focal plane. To determine the energy of the proton beam, the magnetic rigidity of the spectrograph orbit was calibrated by leaving the field strength unchanged and passing a monoenergetic heavy-ion beam of cesium or potassium around the same constrained orbit. That heavy-ion beam was produced by

surface ionization and then accelerated through a potential V , which was adjusted until the ions were observed just upstream from the target. Finally, the optimized voltage V was compared with a 1-volt standard via two successive stages of resistive division. The threshold determined from a yield curve was thus based firmly on a primary calibration standard – the volt – independent of any secondary reaction Q values. However it did require corrections for finite energy spread of the beam, for non-uniform proton energy loss and for atomic excitation. It was also subject to near-threshold resonances, which, if present, could misguide the analysis [23, 18]. Nevertheless, at its apotheosis, this technique achieved a precision of $\sim 2 \times 10^{-5}$ on several measured Q_{EC} values.

2.1.2. Combined (p,γ) and (n,γ) reactions A second reaction-based approach that ultimately led to very precise results was to measure both (p,γ) and (n,γ) reactions on a common target, which had been chosen so that the (p,γ) reaction would produce the parent of a $0^+ \rightarrow 0^+$ β decay, and the (n,γ) reaction would produce the daughter: for example, $^{25}\text{Mg}(p,\gamma)^{26m}\text{Al}$ and $^{25}\text{Mg}(n,\gamma)^{26}\text{Mg}$ [24]. In such cases, the reaction Q values yield Q_{EC} through the relation

$$Q_{EC} = Q_{n\gamma} - Q_{p\gamma} - 782.347 \text{ keV}, \quad (3)$$

which is independent of the mass of the target nucleus.

Continuing with the same example [24], the $^{25}\text{Mg}(n,\gamma)^{26}\text{Mg}$ reaction was studied with thermal neutrons from the Los Alamos Omega West reactor. Gamma rays were detected with a Compton-suppressed Ge(Li) detector, and their energies precisely determined from a calibration based on well known lines observed in the $^1\text{H}(n,\gamma)$, $^{12}\text{C}(n,\gamma)$ and $^{14}\text{N}(n,\gamma)$ reactions. The value of $Q_{n\gamma}$ was then obtained from the average summed energy of a number of γ -ray cascades de-exciting the capture state in ^{26}Mg . For the $^{25}\text{Mg}(p,\gamma)^{26m}\text{Al}$ reaction a dual Mg-Al target (upper half Mg, lower half Al) was employed, over which a proton beam from the Utrecht 3 MV Van der Graaff accelerator was wobbled up and down. The proton energies at four $^{25}\text{Mg}(p,\gamma)^{26m}\text{Al}$ resonances were compared with four accurately known resonances in the $^{27}\text{Al}(p,\gamma)^{28}\text{Si}$ reaction. The proton beam was scanned in 200-eV steps over each ^{25}Mg resonance and its nearest neighbour ^{27}Al resonance, which in all four cases was only a few keV away. Thus each of the proton energy differences could be determined precisely and an average $Q_{p\gamma}$ -value obtained. Obviously this method for determining Q_{EC} depended on secondary calibration standards but it was less dependent on experimental corrections than was the (p,n) reaction described in Sec. 2.1.1. At its best, it achieved a relative precision of $3\text{--}5 \times 10^{-5}$.

2.1.3. Relative $(^3\text{He},t)$ reactions Like (p,n) , a $(^3\text{He},t)$ reaction acting on the daughter of a superallowed $0^+ \rightarrow 0^+$ decay produces the parent of the decay, so the reaction Q value is directly related to Q_{EC} . In contrast with (p,n) though, the energy of the outgoing particle – a tritium ion – can be measured conveniently. Even so, to determine the Q value, the energies of both the tritons and the ^3He projectiles must still be calibrated at

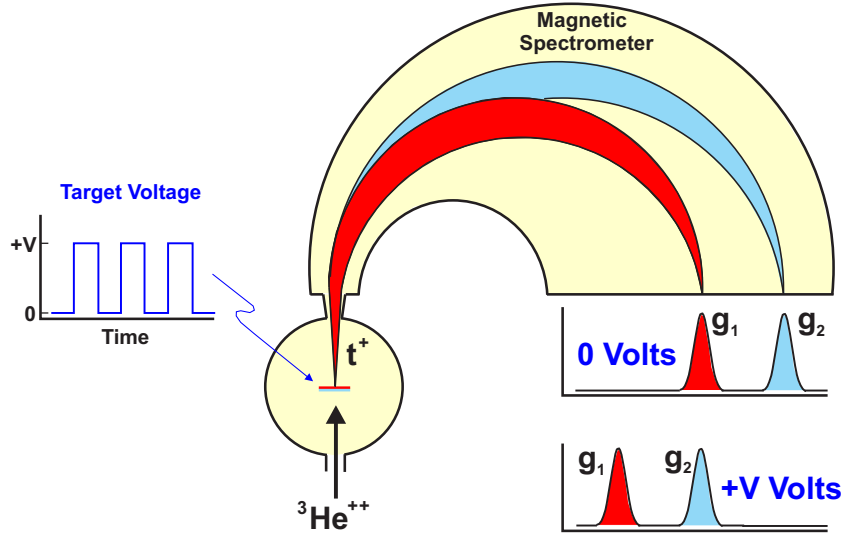


Figure 3. Schematic diagram illustrating the principle of biasing a two-component target in order to peak-match the reaction-product group g_1 from one component with group g_2 from the other component. (Adapted from ref. [25].)

high precision against an established energy standard, not an easy task at the energies involved. Koslowsky, Hardy and collaborators at Chalk River dealt with this difficulty by developing a novel system that allowed them to measure the Q -value differences between two (${}^3\text{He}, t$) reactions produced concurrently from a target containing two components, each the daughter of a superallowed β emitter [25].

Their method is illustrated in Fig. 3. A two-component target was bombarded by a doubly ionized ${}^3\text{He}$ beam of 20-30 MeV from an MP Tandem accelerator. The ejected tritons were analyzed at 0° by a high-resolution Q3D magnetic spectrometer, which transformed their energy spectrum into a distribution in position along its focal plane. The target assembly was constructed so that it could be intermittently biased at +V volts relative to its grounded surroundings, with V being adjustable up to 150 kV. With the target at voltage +V, the ${}^3\text{He}$ beam, being doubly ionized, was retarded by $2V$ eV, while the singly-charged tritons were re-accelerated by only V eV. As a result, the net effect of the imposed voltage was to reduce the triton energy by V eV relative to its value with no voltage on the target, thus shifting its position on the focal plane. The target voltage could then be adjusted until the shifted position of triton group g_2 exactly coincided with the unshifted position of g_1 (see Fig. 3). That adjusted voltage, which was related by resistive division to the standard volt, corresponded to the energy difference between groups g_1 and g_2 . Furthermore, since the shifted tritons (g_2) followed the same path as the unshifted ones (g_1), the result was independent of that path. With g_1 chosen to be a triton group from one target component and g_2 being from the other, the difference between reaction Q values could be precisely determined with reference to the standard volt.

Of course, the superallowed Q_{EC} -value differences themselves were not 150 keV or less. In practice, for each doublet, the experimental team determined the Q -value

difference for the population of an excited state in each of the two β -decay parents, these states being chosen so that their Q -value difference was indeed within 150 keV. Their excitation energies were either known or determined separately via γ -ray spectroscopy, so the measured reaction Q -value differences could be related quite precisely to the superallowed Q_{EC} -value differences. Four pairs of superallowed decay energies were studied in this way [25]. Being differences, the results do not appear in Fig. 2, but their precision was comparable to the best reaction results that do appear there, and they continue to figure prominently in the world averages for Q_{EC} values [9].

2.1.4. Penning-trap mass measurements The Q_{EC} value for β decay is simply the atomic mass difference between the parent state and its daughter: It could be derived from those masses if they were known precisely enough. So far, though, we have just described methods for measuring the difference directly since, until recently, this approach yielded the only precise results. As explanation, consider the superallowed $0^+ \rightarrow 0^+$ decay, $^{26m}\text{Al} \rightarrow ^{26}\text{Mg}$. The masses of the nuclear states in this case are $\sim 2.4 \times 10^{10}$ eV and the difference between them (Q_{EC}) is $\sim 4.2 \times 10^6$ eV. Reaction measurements yield Q_{EC} -values with relative precision of $\sim 3 \times 10^{-5}$ (see Fig. 2), which is ~ 120 eV in this case. To achieve the same precision with a pair of mass measurements would require them each to have a relative precision of $\sim 4 \times 10^{-9}$. This was beyond the capability of conventional mass spectrometry, which in any case was limited to effectively stable nuclei.

The balance has shifted with the appearance of Penning traps coupled on-line to an accelerator. The Penning trap itself can confine charged particles to a small volume by means of static magnetic and electric fields, the former being homogeneous and the latter quadrupolar. The trapped ions exhibit three eigenmotions: one along the axis of the magnetic field, and the other two in the radial plane perpendicular to that axis. By combining the frequencies of these three eigenmotions, one can obtain the cyclotron frequency, ν_c , of the trapped ions and, from it, the mass of the ion itself since

$$\nu_c = \frac{qB}{2\pi m}, \tag{4}$$

where q and m are the charge and mass of the ion, and B is the magnetic field. For stable nuclei, the frequency can be determined via external circuitry, without the trapped ions being released [26]. A relative precision of $2\text{-}3 \times 10^{-12}$ has been achieved this way for the stable nuclei, ^{32}S and ^{31}P , for example [27].

However, the parent nuclei of the superallowed decays – and sometimes the daughters as well – have short half-lives, from a few seconds down to a few tens of milliseconds. This requires a number of additional steps in the experimental procedures. First the ions of interest must be produced by an accelerator; next they are cooled, bunched and if necessary purified; and then they are injected into the Penning trap. Because of the short half-life of the ions, this cycle is repeated continuously with fresh ion bunches being delivered every few seconds. In each cycle, once the ions are trapped, the cyclotron frequency in the trap is probed with an applied radiofrequency

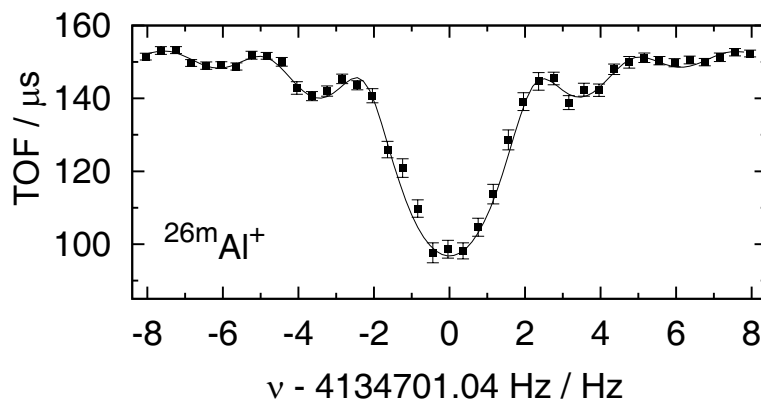


Figure 4. Time of flight (TOF) resonance measured with an on-line Penning trap for the superallowed emitter ^{26m}Al , which has a half-life of 6.3 s. The solid curve is a fitted function. (Adapted from ref. [28].)

electric field, after which the ions are released and their time of flight measured to a microchannel-plate detector located outside the high-field region. As the applied frequency is scanned through the cyclotron frequency, the ions' time-of-flight passes through a distinct minimum, as is shown in Fig. 4. To this basic technique numerous refinements have been applied, the most significant of which is to excite the ion motion with Ramsey's method of time-separated oscillatory fields [29].

On-line Penning trap measurements for superallowed β decay have been, and are being performed at four different facilities: ISOLTRAP (*e.g.* Ref. [30]), CPT (*e.g.* Ref. [31]), LEBIT (*e.g.* Ref. [32]) and JYFLTRAP (*e.g.* Refs. [16, 17]). An early high-impact measurement made with the CPT Penning trap was of the Q_{EC} value for the decay of ^{46}V [31]. The result, which was determined with an uncertainty of ± 400 eV, differed by 2.5 keV from a long-trusted 1977 ($^3\text{He}, t$) reaction measurement that had claimed a similar precision. The latter measurement was based on a "precision time-of-flight measuring system" with the Q3D spectrograph at the Munich Tandem Laboratory; it was one of seven superallowed Q_{EC} values that appeared in a single publication [33] and had stood unchallenged for nearly 30 years. However, the ^{46}V discrepancy was soon confirmed by a second Penning trap, JYFLTRAP, which also identified similar disagreements with the Munich measurements for three other cases, ^{42}Sc , ^{50}Mn and ^{54}Co [28, 34]. When a repeat ($^3\text{He}, t$) measurement [35], made at Munich in 2009 with much of the same equipment, agreed with the Penning trap results, it was decided to eliminate Ref. [33] from surveyed world data [9]. Fortunately, this was the only significant disagreement found between Penning-trap results and those from earlier reaction measurements. It has since been demonstrated that one can safely combine the results of both types of measurement without including any additional systematic uncertainties [18].

To date, the most precise Penning-trap measurements of superallowed Q_{EC} values have been done by Eronen and collaborators with the JYFLTRAP trap at the University of Jyväskylä, where it is coupled to a cyclotron through their Ion Guide Isotope

Separator On Line (IGISOL) [18]. In addition to all the refinements to achieve high trap precision, this facility has an added advantage: It can produce both parent and daughter nuclei with the same beam. For the case illustrated in Fig. 4, the superallowed emitter ^{26m}Al was produced by the (p,n) reaction at 15 MeV on a target of ^{26}Mg . Ions of ^{26}Mg , which is the β -decay daughter, were also released by elastic scattering of the proton beam. The Q_{EC} value is then given by

$$Q_{EC} = M_p - M_d = \left(\frac{\nu_{c,d}}{\nu_{c,p}} - 1 \right) (M_d - m_e) + \Delta_{p,d}, \quad (5)$$

where M_p and M_d are the parent and daughter masses, and $\nu_{c,p}$ and $\nu_{c,d}$ are their respective measured cyclotron frequencies; m_e is the electron rest mass; and the term $\Delta_{p,d}$ arises from atomic-electron binding-energy differences between the parent and daughter, known to sub-eV accuracy. Since the term $(\nu_{c,d}/\nu_{c,p} - 1)$ in (5) is always $\ll 10^{-3}$ for the superallowed parent-daughter pairs, M_d needs only to be known to few-keV precision in order for its uncertainty to have a negligible impact on the Q_{EC} -value precision.

Recent Q_{EC} measurements with JYFLTRAP interleave parent and daughter frequency measurements by switching automatically back and forth between parent and daughter ions after each complete frequency scan, typically every minute or so. This effectively eliminates any systematic differences that might occur from drifts in the magnetic field for example. As a result, a relative precision of 7×10^{-6} has been achieved in several cases, including the Q_{EC} value for the superallowed branch from ^{38m}K , which was determined to be 6044.223(41) keV [16].

2.2. Half-lives

Precise half-life measurements are deceptively difficult. Problems such as impurity activities, rate-dependent thresholds, dead-time and pile-up effects, as well as statistically flawed analyses, offer no obvious signals of their magnitude, or even of their presence. It is not surprising that many half-life measurements of superallowed emitters have had to be rejected from surveys of world data (see table VII in Ref. [9]).

The superallowed $0^+ \rightarrow 0^+$ transitions we are considering here take place between $T=1$ analogue states. As shown in Fig. 1, the parents are of two types: either odd- Z -odd- N nuclei with $T_Z=0$, or even-even ones with $T_Z=-1$. The two types exhibit quite different decay patterns, as is shown in Fig. 5, where $^{38m}\text{K} \rightarrow ^{38}\text{Ar}$ is an example of the first type and $^{38}\text{Ca} \rightarrow ^{38}\text{K}$ is an example of the second. Not surprisingly, most of the best-measured decays in the past have been of $T_Z=0$ nuclei, where the superallowed branch is overwhelmingly predominant. For such cases the only way to measure the half-life is to detect the emitted positrons (or possibly the 511-keV annihilation radiation). However, for the decays of $T_Z=-1$ nuclei – two of which are the classic cases of ^{10}C and ^{14}O , discussed in the Introduction – the total β -decay strength is spread over a number of branches and ample β -delayed γ rays are produced. In these cases half-life measurements based on γ -ray detection have been reported as well as those in which

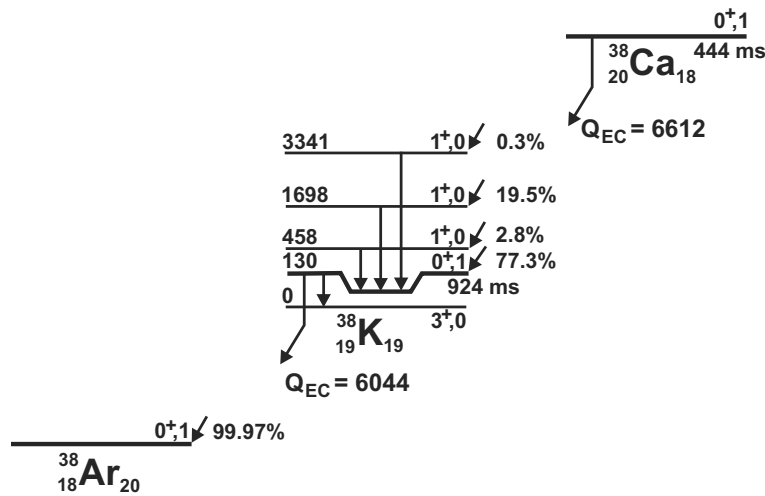


Figure 5. Partial decay schemes of ^{38}Ca and ^{38m}K .

only positrons were recorded. We will briefly describe both measurement techniques with their advantages and disadvantages.

2.2.1. Beta detection methods Direct detection of decay positrons can be accomplished with high efficiency, and the signals from the detector – either a plastic scintillator or a gas counter – can be processed safely at quite high rates. Against these advantages must be balanced the disadvantage presented by the positrons’ broad energy distribution, which cannot in general be used to distinguish one decaying nuclide from another. Without some external means of ensuring source purity, a decay measurement can easily be invalidated by the presence of an undetected impurity. Typically, before 1983, activities were produced by low-energy proton beams on enriched targets, a combination that minimized contaminant activities but could not eliminate them entirely. In a few cases, where impurities were identified, their contribution was corrected for (*e.g.* Refs. [36, 37]) but, in most cases, purity was simply a fervent belief. Since 1983 however, with rare exceptions all measurements have employed sources produced via either an on-line isotope separator – first at Chalk River (*e.g.* Ref. [38]) and later at TRIUMF (*e.g.* Ref. [39]) – or the magnetic recoil spectrometer at the Texas A&M cyclotron (*e.g.* Ref. [40]). These devices eliminate or at least minimize impurities, with the recoil spectrometer also being capable of identifying and quantifying any weak impurities that remain.

Although half-life measurements in the past have frequently used plastic scintillators to detect β particles, in all but one of the thirteen cases of superallowed decays that currently contribute to world data [9], the most precise half-life measurements have all been made with 4π gas proportional counters, all built from the design first developed for this purpose by Koslowsky, Hagberg and Hardy at Chalk River 30 years ago [38]. It was modeled after the “pill box” detectors long used by radiation metrologists [41], chosen because they have low background and are nearly 100% efficient for β particles, while

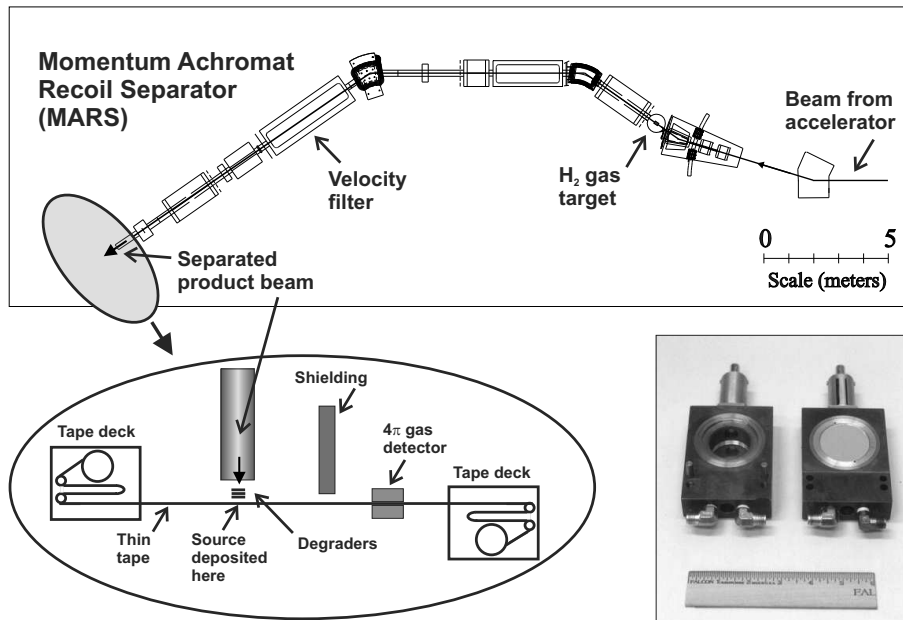


Figure 6. Simplified experimental arrangement used, for example, in measuring the half-lives of ^{38}Ca [42] and ^{46}V [40]. The two halves of the 4π gas proportional counter are pictured at the bottom right. In operation, each half is sealed with a Havar window (as shown on the right half only) and the two halves are bolted together with the Havar windows facing one another. There is a thin slot that remains so the tape can pass between the windows.

being insensitive to γ rays. The detector consists of two separate gas cells machined from copper (as pictured in Fig. 6), each containing an anode of gold-plated tungsten wire $13\ \mu\text{m}$ in diameter, and each hermetically sealed by a Havar window $3.7\ \text{cm}$ in diameter and $1.5\ \mu\text{m}$ thick. Methane at just above atmospheric pressure is continuously flushed through both cells. When assembled together, there is a 25-mm slot between the two cell windows, through which a thin tape can slide. The assembled detector is easily held in the palm of one hand.

Though the detector itself is small, the equipment required to deliver a clean source into the detector is not. In the experimental configuration employed at Texas A&M (see top and left side of Fig. 6) the activity of interest is first produced by bombardment of a cooled hydrogen gas target. Taking the superallowed parent ^{46}V ($t_{1/2} = 423\ \text{ms}$) as an example [40], the activity was produced from the $^1\text{H}(^{47}\text{Ti}, 2n)^{46}\text{V}$ reaction initiated by a 1.5-GeV beam of ^{47}Ti from the K500 cyclotron. The fully stripped reaction products exiting the gas cell entered the Momentum Achromat Recoil Spectrometer (MARS) [43], where they were separated according to their charge-to-mass ratio q/m , with ^{46}V being selected by slits in the focal plane. A position-sensitive silicon detector was periodically inserted at the focal plane to identify and monitor any weak contaminants that were also passing through the slits.

The purified ^{46}V beam was extracted into air, degraded and implanted into the $76\text{-}\mu\text{m}$ -thick aluminized Mylar tape of a fast tape-transport system. The combination of

q/m selectivity in MARS and range sensitivity in the degraders led to collected samples of radioactive ^{46}V , in which the only interfering activity was determined to contribute less than 0.012% to the total. After a sample had been collected for 0.5 s, the beam was turned off and the tape moved the sample 90 cm into the center of the shielded 4π gas detector, where it stopped less than 200 ms later. Signals from the detector were then multiscaled for 10 s, which is more than 20 half-lives of ^{46}V . This cycle was repeated many thousands of times until the desired statistics had been reached.

In all measurements of this type, the counting electronics impose a well-defined non-extendable dead time. This dead time as well as other measurement parameters, such as detector bias and discriminator levels, are altered from time to time in order to test for possible systematic effects. Careful analysis and fitting procedures are applied and these procedures are checked with hypothetical data, computer-generated by Monte Carlo techniques to simulate closely the experimental counting conditions.

In recent years this system has also been used to measure the half-lives of $T_Z = -1$ superallowed parents such as ^{38}Ca (see Fig. 5). There a complication arises: The β decay of the $T_Z = -1$ parent feeds a second superallowed decay, from the $T_Z = 0$ daughter to the $T_Z = +1$ granddaughter. Of course, the positrons from both decays are recorded simultaneously in the β detector. The time-decay spectrum is therefore the sum of the decay of the parent and the growth-and-decay of the daughter. Typically, the parent's half-life is about a factor of two shorter than the daughter's, so the decay of the daughter almost completely masks the decay of the parent (*e.g.* see Refs. [42, 44]). However the composite decay can still be used to determine the parent's half-life if three conditions are met: 1) the half-life of the daughter is known precisely from an independent measurement; 2) the $T_Z = -1$ parent activity deposited on the transport tape is pure; and 3) the rate at which it is deposited is known. The first condition can easily be met by a measurement of the type already described for ^{46}V ; the second is assured by the combination of electromagnetic separation (MARS) and range selectivity; and the third was met by insertion of a thin scintillator into the degrader stack (see Fig. 6), from which the number of ions were recorded as a function of time during sample collection.

With these methods, half-lives with a relative precision of $\sim 0.03\%$ for $T_Z = -1$ parents (*e.g.* ^{26}Si [44]) and $\sim 0.01\%$ for $T_Z = 0$ parents (*e.g.* ^{46}V [40]) have been obtained in the best cases. A result of comparable precision was also obtained for ^{26m}Al at TRIUMF [39], where the same type of gas counter was used but with the sample produced by their isotope separator ISAC. Very recently another measurement of the ^{26m}Al half-life with similar precision has been reported [45], for which digital pulse-analysis was used to process signals from the 4π gas detector instead of analogue electronics. This meant that parameters like dead-time and discriminator level could be investigated, after the fact, on the saved pulse shapes, thus improving the efficiency of data-taking. The relative precision quoted for this measurement was also at the 0.01% precision level, with some promise for future improvement.

2.2.2. Gamma detection methods For a half-life measurement, high-resolution γ -ray detection makes source purity a much less critical requirement, since analysis can focus on the photopeak of a γ ray that is characteristic of the activity of interest. This is the method's principal advantage. On the other side of the ledger must be placed the relatively low efficiency of germanium detectors and the slow signals that are derived from them, with the consequently long time required to process those signals. The latter introduces uncertainties in accounting for dead time and especially for pulse pile-up, which is of course rate dependent. A further disadvantage is that the method can only be applied to $T_Z = -1$ parents of superallowed decays since they are the only ones that produce β -delayed γ rays of sufficient intensity (see Fig. 5).

A recent measurement at TRIUMF illustrates the inherent difficulties with this method. Using a separated beam from the ISAC facility, Laffoley *et al.* [46] measured the half-life of ^{14}O . This nucleus β -decays to ^{14}N with a 99.4% branch to the 2313-keV excited state, which then de-excites by emitting a γ ray to the ground state. The ^{14}O half-life can then be measured through detecting either γ rays or β particles. Laffoley *et al.* did both simultaneously. They implanted ^{14}O from ISAC into thin aluminum at the center of the “ 8π ” γ -ray spectrometer, a spherically symmetric array of 20 HPGe detectors. A fast plastic scintillating detector was placed immediately behind the implantation location to detect β particles. The γ -ray data (for the 2313-keV transition) were carefully analyzed with well worked-out techniques [47] to account for pile-up and other time-dependent effects. The β signals were handled in a very similar way to that used with a gas proportional counter. The results are revealing: The half-life obtained from γ counting was $70.632 \pm 0.086_{stat} \pm 0.037_{syst}$ s, while from β counting it was $70.610 \pm 0.020_{stat} \pm 0.023_{syst}$ s. Though the two measurements were made simultaneously on the same collected sources, both the statistical and systematic uncertainties were larger when γ -rays were employed. Happily though the two results agreed with one another well within their quoted uncertainties.

2.3. Branching ratios

Of the three experimental quantities – Q_{EC} values, half-lives and branching ratios – needed to obtain an ft value, the most difficult to measure precisely is the branching-ratio. Since the continuous energy distribution of emitted positrons leaves little opportunity to distinguish one transition from another, such measurements must be based on detection of the β -delayed γ rays emitted from levels populated in the β -decay daughter. To make matters more difficult, in most cases one of the β transitions populates the ground state or an isomeric state, from which no γ -ray signal is forthcoming. Thus it is not enough to measure the relative branching to excited states. What is needed is the absolute branching for each transition: *i.e.* the fraction each accounts for out of the total decays of the parent nucleus.

What are the competing transitions? Since the parents of our decays of interest have spin-parity 0^+ , they can populate 1^+ states in the daughter by allowed Gamow-

Teller decay, in addition to populating the analogue 0^+ state by the superallowed (Fermi) branch. Furthermore, weak Fermi branches are also possible to excited 0^+ states via charge-driven mixing with the analogue state. The nuclear structure of the daughter nucleus and the energy available for the parent's β decay together determine how many such states can be populated.

Here again the challenges are different for the decays of $T_Z = 0$ superallowed parents compared to the $T_Z = -1$ cases. The superallowed branch from each $T_Z = 0$ parent carries $>99\%$ of the decay strength and populates the ground state of its daughter (see Fig. 5). To determine its exact branching ratio, all that is required is to measure the weak competing branches, if any, with modest precision and subtract their total from 100%. Since the absolute value of the uncertainty on the total of the weak branches becomes the uncertainty on the superallowed branch, a poor relative precision on the former becomes a very good relative precision on the latter. For example, the decay of ^{42}Sc includes a single competing Gamow-Teller β -decay branch to the 1.84-MeV state in ^{42}Ca . Its branching ratio, based on four separate measurements, is 0.0059(14)% [9], a result with $\pm 24\%$ relative precision. The superallowed branching ratio obtained from this result is 99.9941(14), which has a relative precision of $\pm 0.0014\%$! Obviously, high precision is not the issue with these measurements. Rather, the difficulty lies in even observing branches with relative intensities that are less than 100 parts per million of the total decay.

The decays of $T_Z = -1$ superallowed parents are quite different. In general they are characterized by much stronger competing Gamow-Teller transitions (see Fig. 5) and, in a few cases, the superallowed branch is not even the strongest transition: In ^{10}C decay, for example, the superallowed branch only accounts for 1.4646(19)% of the total decay strength [9]. In addition, with two exceptions – ^{10}C and ^{22}Mg – all the known cases include decay branches that do not produce a subsequent γ ray. Consequently, absolute branching ratios must be determined, but without nearly the precision improvement factor just described for decays like that of ^{42}Sc . These ratios must therefore be directly determined with $\sim 0.1\%$ precision. Only very recently has it become possible to do so.

2.3.1. $T_Z = 0$ parent decays Because the daughter of a $T_Z = 0$ superallowed parent is an even- Z -even- N nucleus, its excited 1^+ and 0^+ states are at a relatively high excitation energy above the 0^+ ground state, which is strongly populated by the superallowed transition. For the lightest nuclei, with $A \leq 38$, the β -decay energy window is such that none of these excited states is populated, the limit of observation being at ~ 10 parts per million. However, as A increases, the β -decay energy of the parent grows and the level density in the daughter increases; so competing branches become greater in number and in strength. For ^{42}Sc , the lightest emitter for which a non-superallowed β branch has been observed, that branching ratio is 0.0059%; while for ^{74}Rb , the heaviest well-measured case, there are a number of competing branches, which total to a 0.50% branching ratio.

There have been relatively few measurements of these weak non-superallowed

branching ratios, since parts-per-million sensitivity is not easy to achieve. One example is the work of Hagberg and collaborators [48] at Chalk River, who investigated four emitters, ^{38m}K , ^{46}V , ^{50}Mn and ^{54}Co . The first was produced by an (α, n) reaction, the other three by (p, n) reactions, in all cases on isotopically enriched targets. A helium-jet gas-transfer system was used to convey each activity to a low-background counting location where the activity-loaded NaCl aerosol clusters in the helium were deposited onto the aluminized Mylar tape of a fast tape-transfer system. After a short collection period, typically ~ 0.5 s, a paddle was inserted between the helium-jet nozzle and tape, and the tape moved the sample in sequence to two different detector stations, stopping at each; then the cycle was repeated until adequate statistics had been acquired. To achieve the required sensitivity, MBq-level sources were required for each cycle.

The first detector station consisted of two thin plastic scintillators located on either side of the tape, with an HPGe detector in close geometry behind one of them. The latter was passively shielded against the high flux of energetic positrons from the dominant ground-state branch. Gamma-ray signals from the HPGe detector were only recorded if they were in coincidence with β signals from the opposite-side scintillator and in anti-coincidence with those from the same-side scintillator. This singled out true β -delayed γ rays while eliminating bremsstrahlung radiation in the HPGe detector caused by β particles backscattering from the opposite-side plastic.

At the second detector station the tape stopped in the center of a 4π gas proportional counter (see Sec. 2.2.1) with nearly 100% efficiency for β particles. The multiscaled data from this detector were used to determine the strength of the source in each cycle. With the total strength known, the branching ratio corresponding to any γ -ray peak observed in the HPGe spectrum could be obtained. The HPGe detector efficiency was calibrated with standard sources and there were also significant dead-time and other corrections to be applied so only $\sim 10\%$ relative precision could be quoted on the result but, because the transitions were so weak in the first place, that was more than sufficient. Portions of the γ -ray spectra they recorded from ^{38m}K and ^{46}V are shown in Fig. 7. The arrows indicate where γ rays from known excited 0^+ states would appear if those states were populated by β decay. An upper limit of 19 ppm was obtained for this possible non-superallowed branch from ^{38m}K , and a value of 39(4) ppm was derived from the clearly observed peak in the case of ^{46}V . Results were also obtained for ^{50}Mn and ^{54}Co .

The situation becomes much more complex for $T_Z = 0$ parents with $A \geq 62$. This is well illustrated by the work of Finlay *et al.* [49] at TRIUMF, who studied the β decay of ^{62}Ga . They identified 30 β -coincident γ rays, which they attributed to non-superallowed β transitions from ^{62}Ga to 10 excited 0^+ or 1^+ states in its daughter ^{62}Zn . To obtain this result they deposited ^{62}Ga ions from the ISAC separator onto aluminized Mylar tape at the mutual centers of an array of 20 thin plastic scintillators with $\sim 80\%$ efficiency for β detection, and the “ 8π ” γ -ray spectrometer, an array of 20 HPGe detectors operated in Compton-suppressed mode. Although data were recorded continuously, the beam was cycled on and off, with an implantation period lasting 30 s sandwiched between two

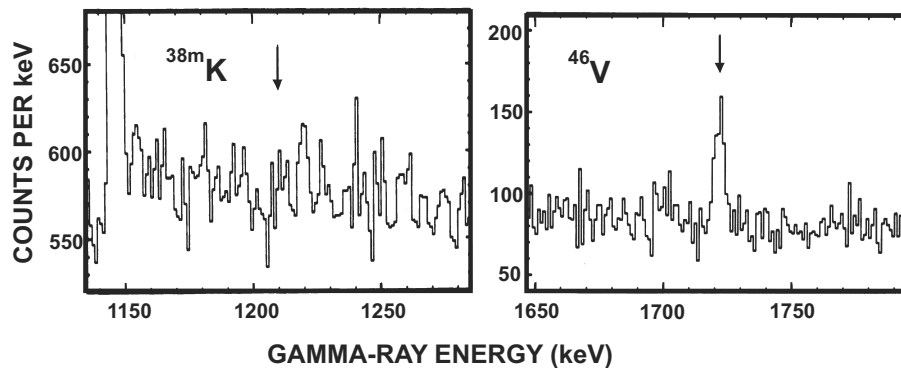


Figure 7. Portions of gated γ -ray spectra obtained following β decays of ^{38m}K and ^{46}V [48]. The position of the possible $0_1^+ \rightarrow 2^+$ γ ray is indicated with an arrow in both cases. The strong peak in the ^{38m}K spectrum is the double-escape peak from the 2168-keV γ ray from the β decay of the ^{38}K ground state. (Adapted from ref. [48].)

shorter periods: one before for background counting, and one after for decay counting. At the end of each cycle, a tape-transport system moved the collected sample to a shielded location, leaving a fresh portion of tape for the next cycle. More than 5000 cycles were recorded in all.

While this thorough experiment might seem to have quantified all possible decay branches, actually it cannot. For these higher A values, hundreds or even thousands of 1^+ states in the daughter can become accessible to β^+/EC decay. Although most of these transitions are undoubtedly very weak, their aggregate can be quite significant at the level of precision required in these measurements. This is the “Pandemonium” effect, which was first described in 1977 in a more general context [50] and, more recently, has been applied specifically to superallowed β decay [51]. In the case of ^{62}Ga decay, shell-model calculations predict that over a hundred 1^+ states in ^{62}Zn can be populated by β decay [49]. With only 10 identified, Finlay *et al.* had to make a correction to their result to account for transitions that they could not observe individually. Their approach hinged on two low-lying 2^+ states in ^{62}Zn , which cannot be populated by allowed β decay yet were seen to have more γ -ray intensity de-populating them than feeding them. The missing feeding could only be attributed to the presence of a large number of γ -ray transitions, each too weak to observe, from excited states fed by correspondingly weak Gamow-Teller β transitions. After a further adjustment from a comparison with theory, they concluded that their detailed spectroscopy had only identified $\sim 94\%$ of the non-superallowed β intensity, and they corrected their result accordingly, arriving at a final superallowed branching ratio of $99.858(8)\%$.

2.3.2. $T_Z = -1$ parent decays As described in the Introduction, the first $T_Z = -1$ parent decays to be studied were those of ^{10}C and ^{14}O . Each has its own unique problem that even today limits the precision with which its branching ratio can be measured. The decay scheme of ^{10}C is shown on the left side of Fig. 8. Since β decay to the 3^+ ground state is second forbidden and decay to the 1^+ state at 2.154 MeV is energetically

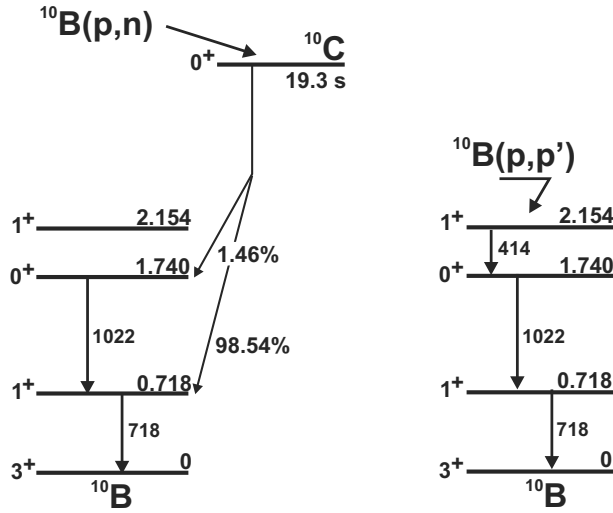


Figure 8. Left: Decay scheme of ^{10}C , which is produced by the $^{10}\text{B}(p,n)$ reaction. Right: Main de-excitation route for the 2.154-MeV level in ^{10}B populated by inelastic proton scattering on ^{10}B . The level energies are given in MeV; the γ -ray energies are in keV.

disfavoured, the superallowed branching ratio is simply given by the ratio of the number of γ rays emitted at 1022 keV relative to the number at 718 keV. There are two problems with this: the superallowed branch is weak and the energy of its characteristic γ ray is exactly twice that of the 511-keV annihilation radiation, which appears in abundance from the decay positrons. Precision requires high statistics together with confidence that the pile up of annihilation radiation has not contaminated the peak of interest. These two conditions tend to work against one another.

Savard *et al.* at Chalk River [52] dealt with these conflicting demands by using the array of 20 HPGe detectors that constituted the 8π spectrometer. This yielded a twentyfold reduction in 511-511 pile-up compared with a single detector at the same total counting rate. The experiment itself comprised two interleaved measurements. One was a repeated cycle in which the ^{10}C was first produced by the (p,n) reaction on a ^{10}B target mounted at the center of the spectrometer; then the beam was interrupted and the β -delayed γ rays from the decay were observed in singles mode. The second measurement was performed in beam with γ - γ coincidences recorded from the deexcitation of the 2.154-MeV level in ^{10}B , which was populated by the (p,p') reaction (see right side of Fig. 8). The ratio of the number of γ_{414} - γ_{718} coincidences to γ_{414} - γ_{1022} coincidences in the second measurement determines the relative counting efficiencies for the 718- and 1022-keV γ rays, which can then be used to determine the relative γ -ray intensities in the first measurement. In this way the superallowed branching ratio was determined to be 1.4625(25)%. Subsequently, a similar measurement was made with the Gammasphere detector array [53], which gave a slightly less precise, but nevertheless consistent result.

The decay of ^{14}O has an even more challenging feature. The superallowed branch carries more than 99% of the decay strength and populates the analogue state at 2.31 MeV in ^{14}N . However, its strongest competition comes from a 0.6% Gamow-Teller branch

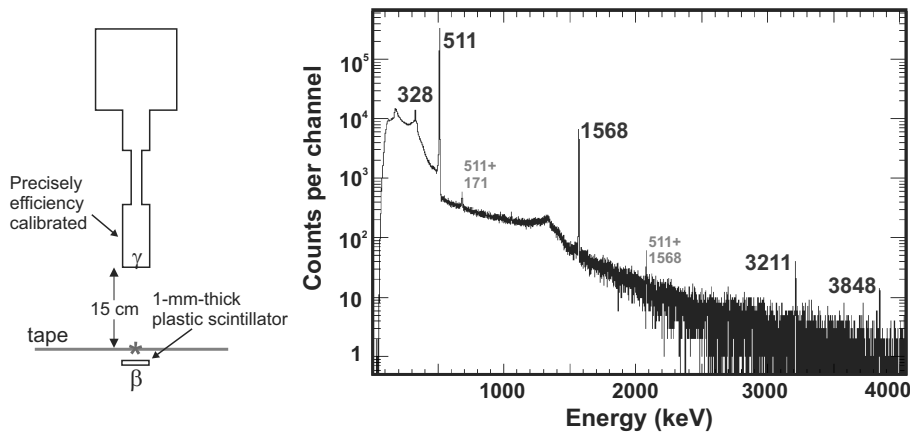


Figure 9. Left: Arrangement of the β and γ -ray detectors, between which the source is placed by the tape transport system illustrated in Fig. 6. Right: Spectrum of β -coincident γ rays recorded from 61,000 cycles, each having a 1.54-s counting period [56].

to the ground state, which emits no subsequent γ ray to signal its appearance. The only way to determine the precise strength of this ground state β -decay branch is to measure the energy spectrum of all the emitted positrons and tease out the contribution of the ground state branch. The last time this measurement was made was in 1966 [54] (though the analysis was updated more recently [55]). This measurement begs to be repeated.

There are, of course, other $T_Z = -1$ superallowed parents with $A \geq 18$ but, until very recently, their branching ratios have defied $\pm 0.1\%$ measurements since in all cases but one, ^{22}Mg , not every β -decay branch feeds excited states that subsequently emit γ -rays. With the ground state – or a low-lying isomeric state – also populated, the only way to arrive at correct branching ratios is to measure the intensity of the γ -ray peaks relative to the total number of decays of the parent nucleus. A method to achieve this has now been developed at Texas A&M University by Hardy, Iacob and Park [56] using the same source-production and delivery system as illustrated in Fig. 6. For these measurements, though, the gas proportional detector shown in that figure is replaced at the counting station by a thin plastic scintillator on one side of the tape and an HPGe detector on the other side, as shown on the left side of Fig. 9. They record β singles and β - γ coincidences.

If the γ ray de-exciting state i in the daughter is denoted by γ_i , then the β -branching ratio, R_i for the β transition populating that state can be written:

$$R_i = \frac{N_{\beta\gamma_i}}{N_\beta \epsilon_{\gamma_i}} k, \quad (6)$$

where $N_{\beta\gamma_i}$ is the total number of β - γ coincidences measured in the γ_i peak, N_β is the total number of β singles, ϵ_{γ_i} is the HPGe efficiency for detecting γ_i , and k is a small correction factor (*i.e.* $k \sim 1$) that accounts for dead time and pile-up, coincident summing, and the small changes in β -detector efficiency for the different energy transitions participating in the decay. The equation highlights the importance

of having a pure sample – so that N_β can be relied upon – as well as having a precise absolute efficiency calibration for the γ -ray detector, and a reasonable knowledge of relative efficiencies in the beta detector. The key ingredient that the Texas A&M team has painstakingly developed is an HPGe detector whose absolute efficiency has been accurately determined (to $\pm 0.2\%$ for 50-1400 keV γ rays and to $\pm 0.4\%$ up to 3500 keV) from source measurements and Monte Carlo calculations [57, 58].

This method yields the branching ratios of all transitions except the one to the ground (or isomeric) state which has no subsequent γ ray. However, the branching ratio of the latter transition can be obtained by subtracting the sum of the former branching ratios from 100%. In the case of the ^{38}Ca decay, which is shown in Fig. 5, the “missing” transition is the superallowed one, and the subtraction from 100% actually has a very salutary effect on the relative precision, reducing it by more than a factor of 3 ($= 22.7/77.3$). Very recently with this system, the branching ratio for the ^{38}Ca superallowed transition has been determined to $\pm 0.2\%$ [56]. This completes the information needed to obtain a precise ft value for this transition and will add ^{38}Ca to the current list of well known superallowed decays (see Fig. 1), the first to be added in nearly a decade. There will likely be several more additions of this type in the next few years.

2.4. Survey of world data

Many independent measurements contribute to the determination of superallowed ft values, so for the past four decades we have periodically produced critical surveys of relevant world data available at the time of writing. All published measurements are carefully considered, with some being rejected but only if a specific fault has been identified. Of the surviving results, only those with uncertainties that are within a factor of 10 of the most precise measurement for each quantity are retained. They are then averaged by the same procedures as those adopted by the Particle Data Group [10]. In columns two, three and four of table 1 we present the results from the most recent survey [9]. In almost all cases, the tabulated values are averages of several – sometimes many – experimental measurements with comparable uncertainties.

For each superallowed transition, the three measured quantities, Q_{EC} , $t_{1/2}$ and R , together with a small correction ($\sim 0.1\%$) [9] to account for the contribution of electron capture, are combined to obtain an ft value. These ft values appear in column five of the table. The next step is to use (2) to obtain the corrected $\mathcal{F}t$ value for each transition. Before doing this though, we need to examine the theoretical correction terms used to account for radiative and isospin-symmetry-breaking effects.

3. Theoretical corrections

3.1. Radiative corrections

As described in the Introduction, the historical determination of the vector coupling constant G_V in the semi-leptonic decays of ^{14}O and ^{10}C differed by a few percent from

Table 1. Experimental results (Q_{EC} , $t_{1/2}$ and R) and calculated corrections terms discussed in the text (δ'_R , δ_{NS} and δ_C) for the precisely measured $0^+ \rightarrow 0^+$ transitions, together with their derived ft and $\mathcal{F}t$ values [9].

Parent nucleus	Q_{EC} (keV)	$t_{1/2}$ (ms)	R (%)	ft (s)	δ'_R (%)	δ_{NS} (%)	δ_C (%)	$\mathcal{F}t$ (s)
^{10}C	1907.87(11)	19308(4)	1.4646(19)	3042(4)	1.679(4)	-0.35(4)	0.175(18)	3076.7(46)
^{14}O	2831.24(23)	70620(15)	99.37(7)	3042.3(27)	1.543(8)	-0.25(5)	0.330(25)	3071.5(33)
^{22}Mg	4124.55(28)	3875.2(24)	53.16(12)	3052(7)	1.466(17)	-0.225(20)	0.380(22)	3078.0(74)
$^{26}\text{Al}^m$	4232.66(6)	6345.0(19)	>99.997	3036.9(9)	1.478(20)	0.005(20)	0.310(18)	3072.4(14)
^{34}Cl	5491.64(23)	1526.6(4)	>99.988	3049.4(12)	1.44(3)	-0.085(15)	0.65(5)	3070.6(21)
^{34}Ar	6063.0(5)	843.8(4)	94.45(25)	3053(8)	1.423(29)	-0.180(15)	0.67(6)	3069.6(85)
$^{38}\text{K}^m$	6044.40(11)	924.33(27)	99.967(4)	5051.9(10)	1.44(4)	-0.100(15)	0.66(6)	3072.5(24)
^{42}Sc	6426.3(3)	680.72(26)	99.9941(14)	3047.6(14)	1.45(5)	0.035(20)	0.67(6)	3072.4(27)
^{46}V	7052.49(16)	422.59(11)	99.985($^{+1}_{-4}$)	3049.5(9)	1.45(5)	-0.035(10)	0.62(6)	3073.3(27)
^{50}Mn	7634.45(7)	283.21(11)	99.942(3)	3048.4(12)	1.44(6)	-0.040(10)	0.66(5)	3070.9(28)
^{54}Co	8244.37(28)	193.27(6)	99.996($^{+1}_{-30}$)	3050.8($^{+11}_{-15}$)	1.44(7)	-0.035(10)	0.77(7)	3069.9(33)
^{62}Ga	9181.1(5)	116.12(4)	99.862(11)	3074.1(15)	1.46(9)	-0.045(20)	1.48(21)	3071.5(72)
^{74}Rb	10417(4)	64.78(4)	99.50(10)	3085(8)	1.50(12)	-0.075(30)	1.6(3)	3078(13)
Average, $\overline{\mathcal{F}t}$								3072.08(79)
χ^2/ν								0.28

G_F , which was obtained from the purely leptonic decay of the muon – seemingly violating universality as espoused by Cabibbo. At the time though it was understood that radiative corrections could largely explain the discrepancy. Simply put, the lifetimes measured in the decays of ^{14}O and ^{10}C include both the bare β -decay process and the radiative process, in which the emitted electron releases a bremsstrahlung photon that is undetected. Since G_V is determined from the bare β -decay process, the contribution from radiative effects needs to be computed and subtracted from the measured result. Calculations of this contribution, however, have to consider not just the bremsstrahlung process alone but also the loop diagram in which a photon is exchanged between charged particles. The key point is that the bremsstrahlung contribution diverges in the limit when the photon energy goes to zero; the loop graph likewise diverges but with the opposite sign, so the combination of the two remains finite in the low-energy limit. That this happens is a consequence of the renormalizability of quantum electrodynamics.

There was another problem for the calculations performed in the 1950s [59, 60]: the loop graph also diverged in the limit of infinite photon energy, so some form of arbitrary cut-off had to be imposed. The difficulty at the time was what to choose for the cut-off: As the cut-off increased so did the discrepancy between G_V and G_F . In this era the β -decay process was treated as a four-fermion contact interaction and the loop diagram was of triangular geometry.

During the 1960s, the Standard Model began to be formulated and the four-fermion contact interaction was replaced by one in which an intermediate vector boson – the W boson – mediated between the leptons and hadrons in semi-leptonic decay. With the W boson, the loop diagram became of rectangular geometry and the mass of the boson then provided a natural cut-off [61]. The Standard Model also introduced a neutral Z boson that mixed with the photon, so a further class of loop diagrams involving Z -boson

exchange had to be included in the radiative-correction calculation. The main effect of this addition was to increase the effective cut-off in the loop diagram from the W -boson mass to the Z -boson mass [62, 63].

It was realized all along that the purely leptonic muon decay was also subject to radiative corrections and that many of the potential contributions were identical in both pure- and semi-leptonic decays. Such identical contributions are called ‘universal’. Thus, in the Standard Model, G_F came to be defined as the weak-interaction coupling constant, with the understanding that it included within it all universal radiative corrections. Thus, the radiative correction applied to the semi-leptonic decays only needed to include terms that were non-universal. A longer discussion of this point is given by Sirlin [62].

So far, the radiative correction was only calculated to lowest order in the fine-structure constant α . In the 1970s, Jaus and Rasche [64, 65] gave the first estimate of the order- $Z\alpha^2$ contributions, where Z is the charge number of the daughter nucleus. This correction is defined as the contribution at this order not already contained in the product $F(Z, E)(1+\delta_1)$, where $F(Z, E)$ is the Fermi function, E the electron total energy and δ_1 the order- α correction. Also in the 1970s, experimental results of superallowed beta decay began to emerge in the higher- Z elements of ^{42}Sc , ^{46}V , ^{50}Mn and ^{54}Co . These results raised a problem [66]: the high- Z cases seemed to be failing the required Cabibbo universality. This prompted a reexamination of the order- $Z\alpha^2$ radiative correction by Sirlin and Zucchini [67, 68] and Jaus and Rasche [69]. An error was discovered in the earlier work and Cabibbo universality was duly recovered.

In the loop graph there is another interesting wrinkle. If the nucleus is treated as a collection of nucleons, and if the weak and the electromagnetic interactions occurring in the radiative correction interact with the same nucleon, then the graph evaluation leads to a result that is proportional to the expectation value of the isospin ladder operator. Since the bare β -decay process also proceeds via the isospin ladder operator, the radiative correction simply scales with the bare β -decay value. This implies that the calculation is independent of nuclear structure, the result depending only on the electron energy and the charge Z of the daughter nucleus. If, however, the weak and electromagnetic interactions occur with different nucleons, then the scaling property fails and a full nuclear-structure-dependent calculation is required. The first such calculation was provided by Jaus and Rasche [70, 71] and later refined by Towner [72, 73]. These results constitute the δ_{NS} correction, which appears in (2).

Another property of the loop graph is that one can usefully employ different approximations for the hadronic structure depending upon whether the photon energy is small or large. At low photon energy, it is sufficient to treat the nucleus as a collection of nucleons and use nucleon weak and electromagnetic form factors at the vertices. At high photon energy, the hadronic structure is essentially that of a soup of quarks. In this limit, the calculation becomes independent of the details of hadronic structure and leads to the term Δ_R^V in (2). Marciano and Sirlin [74] have critically examined this separation into low- and high-energy contributions and the linkages between them.

Their recommended value for Δ_R^V is in current use:

$$\Delta_R^V = (2.361 \pm 0.038)\%. \quad (7)$$

Lastly, a correction to order α^2 was recently considered by Czarnecki, Marciano and Sirlin [75] and is now included in current computations.

All contributions to the radiative correction considered to date are collated into δ'_R , δ_{NS} and Δ_R^V as displayed in (2). The currently accepted values [76] for δ'_R and δ_{NS} are given in columns six and seven of table 1.

3.2. Isospin symmetry-breaking corrections

The Conserved Vector Current (CVC) hypothesis asserts that the vector coupling constant G_V is not renormalized in the nuclear medium but is the same for all nuclei. This assertion can be tested by the measurement of superallowed β decays, which cover a wide range of nuclei spanning from ^{10}C to ^{74}Rb . However, the CVC hypothesis is only valid in the isospin-symmetry limit, so if we are to determine G_V from a wide range of nuclei then a correction has first to be applied that removes the effects of isospin-symmetry breaking. Isospin symmetry is naturally broken in nuclei because the protons are subject to the Coulomb interaction, which is not felt by the neutrons. Thus, the wave function of a proton in a given quantum state differs slightly from a neutron in the mirror nucleus in the same quantum state. This is reflected in the nuclear matrix element describing the beta-decay transition between mirror states. The isospin symmetry-breaking correction δ_C is defined by the relation

$$|M_F|^2 = |M_F^0|^2(1 - \delta_C), \quad (8)$$

where M_F is the exact Fermi matrix element and M_F^0 its isospin-symmetry-limit value, being just the expectation value of the isospin ladder operator.

One of the earliest estimates of δ_C was provided by Damgaard [77] in 1969. He suggested that the radial function of the proton in beta decay could be expanded in a complete set of neutron radial functions of the same angular momentum; the terms in the set differing in the number of radial nodes in the function. The expansion coefficients were determined in perturbation theory, with the Coulomb force being the perturbing interaction. With the basis states taken as harmonic oscillator functions, Damgaard obtained the expression

$$\delta_C = \frac{Z^2}{(\hbar\omega)^4 r^6} \frac{e^2 \hbar^4}{16m^2} (n+1)(n+\ell + \frac{3}{2}). \quad (9)$$

If one adopts the relationships for the characteristic oscillator energy, $\hbar\omega = 41A^{-1/3}$ MeV, and the nuclear radius, $r = 1.2A^{1/3}$ fm, this expression becomes

$$\delta_C = 0.2645Z^2 A^{-2/3} (n+1)(n+\ell + \frac{3}{2}), \quad (10)$$

which, for the relatively light nuclei we are interested in here, exhibits the general behaviour $\delta_C \propto Z^{4/3}$ with some shell structure superimposed through the choice of oscillator quantum numbers n and ℓ . In particular, a proton radial function with one

radial node gets a factor of 2 enhancement in its δ_C value over one that has no radial nodes simply from the factor $(n + 1)$ in (10). This enhancement is clearly evident in table 1 for the upper pf shell, where there is a significant increase in experimental ft value when going from ^{54}Co ($ft=3051$ s) to ^{62}Ga ($ft=3074$ s).

Beginning in 1973, Damgaard's approach has been improved upon by Towner and Hardy [8, 76, 78, 79] in two significant ways. The oscillator basis states have been replaced by eigenfunctions of a Woods-Saxon potential and the extreme non-interacting single-particle model has been replaced by the interacting shell model. The perturbing Coulomb force is long range and influences a huge number of configurations in the shell model. Thus it has become expedient to divide δ_C into two components

$$\delta_C = \delta_{C1} + \delta_{C2} , \tag{11}$$

where δ_{C1} is a contribution from a finite-sized shell-model calculation, typically containing all configurations within one major shell, while δ_{C2} steps outside that model space to states that typically have a different number of radial nodes influencing the proton and neutron radial functions. For superallowed transitions between the 0^+ states of interest here, Towner and Hardy [76] find that the δ_{C1} contributions are much smaller than the δ_{C2} ones. Their results are shown in table 2, where they are labelled SM-WS. We note that these results are considered to be semi-phenomenological since a number of isospin-specific nuclear properties have been fitted in their derivation: *viz.* the measured proton and neutron separation energies in the parents and daughters, respectively, were used in the calculation of δ_{C2} ; and each calculation of δ_{C1} was tuned to fit the b - and c -coefficients in the isobaric multiplet mass equation corresponding to the specific $T = 1$ multiplet that included the parent and daughter state.

From 1985 to 1995, Ormand and Brown [80, 81, 82] adopted the same general procedure as the one just described but used eigenfunctions of a Hartree-Fock mean field rather than a Woods-Saxon potential. Their results were systematically smaller than the SM-WS values and this difference was used to assess a systematic error in the analysis of superallowed beta-decay data. This systematic difference, however, was much reduced by a 2009 calculation of Hardy and Towner [9], in which the protocol for the Hartree-Fock calculation was altered to ensure that the Coulomb part of the proton mean field obtained from the Hartree-Fock calculation had the appropriate asymptotic form. The results from this calculation are labelled SM-HF in table 2.

Besides Damgaard's model and the two shell-model approaches to δ_C , which apply to the full range of measured superallowed transitions, there have been many other less-complete computations by various authors [83, 84, 85, 86, 87, 88, 89] using a diverse set of nuclear models. There are too many to discuss all these cases here. We have selected two of them, one based on the random phase approximation (RPA) and the other on density functional theories (DFT) to include in table 2. In the former, the RPA work of Sagawa *et al* [83], improved upon by Liang *et al* [84], treats the even-even nucleus of the parent-daughter pair as a core, and the analogue odd-odd nucleus as a particle-hole excitation built on that core. The particle-hole calculation is carried out in the charge-

Table 2. Six sets of δ_C calculations from model approaches labelled Damgaard, DFT, RHF-RPA, RH-RPA, SM-HF and SM-WS (see text). Also given is the chi square per degree of freedom, χ^2/n_d , from the confidence test proposed in ref. [11].

Nucleus	$\delta_C(\%)$					
	Damgaard	DFT	RHF-RPA	RH-RPA	SM-HF	SM-WS
^{10}C	0.046	0.462(65)	0.082	0.150	0.225(36)	0.175(18)
^{14}O	0.111	0.480(48)	0.114	0.197	0.310(36)	0.330(25)
^{22}Mg	0.153	0.432(49)			0.260(56)	0.380(22)
^{26m}Al	0.182	0.307(62)	0.139	0.198	0.440(51)	0.310(18)
^{34}Cl	0.326		0.234	0.307	0.695(56)	0.650(46)
^{34}Ar	0.285	1.08(42)	0.268	0.376	0.540(61)	0.665(56)
^{38m}K	0.370		0.278	0.371	0.745(63)	0.655(59)
^{42}Sc	0.414	0.70(32)	0.333	0.448	0.640(56)	0.665(56)
^{46}V	0.524	0.375(96)			0.600(63)	0.620(63)
^{50}Mn	0.550	0.39(13)			0.620(59)	0.655(54)
^{54}Co	0.613	0.51(20)	0.319	0.393	0.685(63)	0.770(67)
^{62}Ga	1.34				1.21(17)	1.48(21)
^{74}Rb	1.42	0.90(22)	1.088	1.258	1.42(17)	1.63(31)
χ^2/n_d	1.7	1.9	2.7	2.1	2.2	0.4

exchange version of the RPA. The more recent of the two works [84] replaces zero-range interactions with finite-range meson-exchange potentials, and a relativistic rather than nonrelativistic treatment (RHF-RPA) is used. In a variation of this approach, density-dependent meson-exchange vertices were introduced in a Hartree (only) computation with nonlocal interactions (RH-RPA). Both these sets of results are listed in table 2.

Most recently, Satula *et al* [89] used an isospin- and angular-momentum-projected density functional theory (DFT). This method accounts for spontaneous symmetry breaking, configuration mixing and long-range Coulomb polarization effects. The results are also listed in table 2.

The six sets of δ_C values in table 2 show a wide variation. Some yardstick is required to distinguish the quality of one set relative to another, so Towner and Hardy [11] proposed such a test using the premise that the CVC hypothesis is valid. The requirement is that a calculated set of δ_C values should produce a statistically consistent set of $\mathcal{F}t$ values, the average of which we can write as $\overline{\mathcal{F}t}$. Then (2) can be written for each individual transition in the set as

$$\delta_C = 1 + \delta_{NS} - \frac{\overline{\mathcal{F}t}}{ft(1 + \delta'_R)}. \tag{12}$$

For any set of corrections to be acceptable, the calculated value of δ_C for each superallowed transition must satisfy this equation, where ft is the measured result for the transition and $\overline{\mathcal{F}t}$ has the same value for all of them. Thus, to test a set of δ_C values for n superallowed transitions, one can treat $\overline{\mathcal{F}t}$ as a single adjustable parameter and use it to bring the n results for the right-hand side of (12), which are based predominantly

on experiment, into the best possible agreement with the corresponding n calculated values of δ_C on the left-hand side of the equation. The normalized χ^2 , minimized by this process then provides a figure of merit for that set of calculations. The χ^2 for each fit, expressed as χ^2/n_d , where $n_d = n - 1$ is the number of degrees of freedom, is given in the last row of table 2.

The most obvious outcome of this analysis is that the model, SM-WS, has a χ^2 smaller by a factor of five than the other five cases cited. For this reason, the SM-WS δ_C values are the ones used in the calculation of the $\mathcal{F}t$ values, and it is these δ_C values that appear in the eighth column of table 1. However, the other δ_C calculations can be used to help establish a systematic-uncertainty assignment on this analysis.

4. Impact on weak-interaction physics

4.1. The value of V_{ud}

The $\mathcal{F}t$ values obtained with the Woods-Saxon isospin-symmetry breaking correction SM-WS appear in the ninth column of table 1, where all are seen to be mutually consistent. Thus, we are justified in averaging the 13 entries in table 1 and using the result, $\overline{\mathcal{F}t} = 3072.08 \pm 0.79$ s, to determine the CKM matrix element V_{ud} . However, before doing so we must consider the impact that a different set of isospin-symmetry breaking corrections might have on the result. In the past [15], we compared the SM-WS calculations with the Hartree-Fock calculations of Ormand and Brown [80, 81, 82], whose δ_C corrections covered all measured transitions and were consistently smaller than those obtained with Woods-Saxon functions. We considered that this provided a valid estimate of the systematic (theoretical) uncertainty, and so incorporated it into the overall result by deriving two average $\overline{\mathcal{F}t}$ values, one for each set of δ_C calculations, then adopting the average of the two and assigning a systematic uncertainty equal to half the spread between them.

This procedure was continued in the most recent 2009 survey [9], except that the Ormand and Brown calculations were replaced by the Towner-Hardy Hartree-Fock values, SM-HF in table 2. With the SM-HF δ_C values, the average $\overline{\mathcal{F}t}$ value became 3071.55 ± 0.89 s but with a substantially increased chi-square of $\chi^2/\nu = 0.93$. This normalized chi-square is three times what was obtained in table 1 with Woods-Saxon corrections, which arguably could justify a rejection of the Hartree-Fock results outright. However, to be safe, we proceeded as in the 2005 survey and take the average of the SM-WS and SM-HF results, adding a systematic uncertainty equal to half the spread between the two results. Thus, the 2009 survey [9] arrived at

$$\begin{aligned} \overline{\mathcal{F}t} &= 3071.81 \pm 0.79_{\text{stat}} \pm 0.27_{\text{syst}} \text{ s} \\ &= 3071.81 \pm 0.83 \text{ s} , \end{aligned} \tag{13}$$

where on the second line the two uncertainties have been added in quadrature.

With $\overline{\mathcal{F}t}$ thus obtained, the CKM matrix element V_{ud} is derived from a

rearrangement of (1) and (2):

$$|V_{ud}|^2 = \frac{K}{2G_F^2(1 + \Delta_R^V)\overline{\mathcal{F}t}} = \frac{2915.64 \pm 1.08}{\overline{\mathcal{F}t}}, \quad (14)$$

where the overall weak-interaction coupling constant from muon decay is $G_F/(\hbar c)^3 = 1.1663787(6) \times 10^{-5} \text{ GeV}^{-2}$ from Ref. [10] and Δ_R^V is taken from (7). On applying our recommended value of $\overline{\mathcal{F}t}$ from (13) we arrive at

$$|V_{ud}| = 0.97425 \pm 0.00022, \quad (15)$$

a value with 0.02% precision.

This result is certainly the most precise current determination of V_{ud} , but superallowed $0^+ \rightarrow 0^+$ β decay is not the only experimental approach to V_{ud} . Neutron decay, nuclear $T = 1/2$ mirror decays and pion beta decay have all been used for this purpose. For now, these other methods cannot compete with $0^+ \rightarrow 0^+$ decays for precision, although they yield statistically consistent results [11]. We need not consider them farther in this context.

4.2. Unitarity of the CKM matrix

That the sum of the squares of the top-row elements should add to one is the most stringent test of the CKM matrix's unitarity. Here V_{ud} plays the dominant role with by far the largest magnitude and the smallest relative uncertainty; but, when it comes to the unitarity sum, V_{us} and V_{ud} contribute equally to the uncertainty because the terms themselves have such different magnitudes. For V_{us} we will use the value reported at the recent CIPANP 2012 conference [90] (which updates the 2012 Particle Data Group value [10]):

$$|V_{us}| = 0.2256 \pm 0.0008. \quad (16)$$

This value is an average of results obtained from kaon semi-leptonic decays, $K_{\ell 3}$, of both charged and neutral kaons, and from the purely leptonic decay of the kaon, $K_{\ell 2}$. Both methods rely on lattice QCD calculations for values of the hadronic form factors. Other determinations from hyperon decays and hadronic tau decay do not have the precision at the present time to challenge the results from kaon decays.

The third element of the top row of the CKM matrix, V_{ub} , is very small and hardly impacts on the unitarity test at all. Its value from the 2012 PDG compilation [10] is

$$|V_{ub}| = (4.15 \pm 0.49) \times 10^{-3}. \quad (17)$$

Combining the values given in (15), (16) and (17), the sum of the squares of the top-row elements of the CKM matrix becomes

$$\begin{aligned} |V_{ud}|^2 + |V_{us}|^2 + |V_{ub}|^2 &= 1.00008 \pm 0.00043_{V_{ud}} \pm 0.00036_{V_{us}}, \\ &= 1.00008 \pm 0.00056, \end{aligned} \quad (18)$$

a result that shows unitarity to be fully satisfied at the 0.06% level. In the first line of (18), the two errors shown are firstly from the uncertainty in V_{ud} and secondly from

V_{us} . They are combined in quadrature in the second line. Observe that kaon decays contribute slightly less than nuclear decays to the error budget.

No other row or column approaches this precision on a unitarity test. The first column comes closest, with $|V_{ud}|^2 + |V_{cd}|^2 + |V_{td}|^2 = 1.0021 \pm 0.0051$ [91], but this is a factor of ten less precise than the top-row sum. The corresponding sums for the second row and second column are 1.067 ± 0.047 and 1.065 ± 0.046 respectively [91], another order of magnitude less precise. Without question the top-row sum provides the most demanding test of CKM unitarity, V_{ud} is its dominant contributor, and superallowed β decay is effectively the sole experimental source for the value of V_{ud} .

The excellent experimental agreement with unitarity provides strong confirmation of the Standard-Model radiative corrections that enter both nuclear and kaon decays at the 3 to 4% level and, to a lesser extent, confirmation of isospin-symmetry breaking estimates, again in both nuclear and kaon decays. In addition it implies constraints on new physics beyond the Standard Model. New physics can enter in one of two ways: directly, via a new semi-leptonic interaction (*e.g.* scalar currents or right-hand currents), or indirectly, via loop-graph contributions to the radiative corrections (*e.g.* extra Z bosons). Discussions of these issues can be found in [11, 92, 93] as well as in other contributions to this volume.

5. Future Prospects

Because the unitary CKM matrix is an essential pillar of the Standard Model, the uncertainty limits on the unitarity sum in (18) constrain the scope of whatever new physics may be anticipated to lie beyond that model. Consequently, there is ample motivation to search for improvements in both theory and experiment that can reduce the uncertainty on the sum, and potentially expose – or rule out – some classes of new physics.

Currently the uncertainty in the value of V_{us} is dominated by the lattice QCD estimate for the form factor used to extract it from the experimental measurements on $K_{\ell 3}$ decays. It is predicted, though, that these lattice calculations will improve considerably over the next decade, with reasonable prospects of reducing the V_{us} uncertainty by a factor of 2 [90, 12]. With this improvement in sight, it is evident from (18) that any future improvements in V_{ud} will thus have a significant impact on the overall uncertainty of the unitarity sum. Are such improvements foreseeable?

It is the uncertainties on the calculated correction terms, particularly Δ_R^V , δ_C and δ_{NS} , that have the greatest influence on the uncertainty of V_{ud} . The largest contributor, Δ_R^V , may be open to some improvement, with a 30% reduction in uncertainty having been suggested as possible [94]. This is a challenge exclusively for theorists. However, improvements in the nuclear-structure-dependent corrections, δ_C and δ_{NS} , can actually be achieved with the help of experiments. As described in Section 3.2, these terms are subject to a test: They can be applied to the uncorrected experimental ft values to obtain a set of $\mathcal{F}t$ values, which can then be evaluated for the consistency required by

CVC – see (12) and table 2. The more precisely the ft values have been measured, the more demanding this test can be; and if new superallowed transitions with larger predicted nuclear corrections can be measured, the test will be improved still more.

Of particular importance in this context are superallowed $0^+ \rightarrow 0^+$ decays of the $T_Z = -1$ nuclei ^{26}Si , ^{34}Ar , ^{38}Ca and ^{42}Ti . As noted in Section 2.3.2, these decays are more complex than the currently well studied superallowed transitions, which mostly have $T_Z = 0$ parents. Only very recently have $T_Z = -1$ decays in this mass region become amenable to precise ft -value measurements [56] and it is anticipated that all four will be fully characterized within the next few years. These cases will be influential not only because they have relatively large nuclear corrections but also because each of the four transitions is mirror to another well known transition, ^{26m}Al , ^{34}Cl , ^{38m}K and ^{42}Sc , respectively. It turns out that the ratio of the ft -values for mirror superallowed transitions is extremely sensitive to the model used to calculate δ_C and δ_{NS} [56]. There is good reason to expect that these new cases will tighten the model constraints enough to shrink or even remove entirely the systematic uncertainty now applied to the structure-dependent correction terms.

The potential improvements in all the correction terms should act to reduce the uncertainty in V_{ud} by about 25% and, together with the improvements expected in V_{us} , can be expected to reduce the uncertainty in the CKM unitarity sum – see (18) – from ± 0.00056 to ± 0.00037 . This is likely to be the extent of possible improvements in the foreseeable future.

Acknowledgments

This work was supported by the U.S. Department of Energy under Grant No. DE-FG03-93ER40773 and by the Robert A. Welch Foundation under Grant No. A-1397.

References

- [1] Sherr R and Gerhart J B 1953 *Phys. Rev.* **91** 909
- [2] Sherr R, Murther H R and White M G 1949 *Phys. Rev.* **75** 282
- [3] Bardin R K, Barnes C A, Fowler W A and Seeger P A 1960 *Phys. Rev. Lett.* **5** 323
- [4] Sherr R, Gerhart J B, Horie H and Hornyak, W F 1955 *Phys. Rev.* **100** 945
- [5] Feynman R P and Gell-Mann M 1958 *Phys. Rev.* **109** 193
- [6] Cabibbo N 1963 *Phys. Rev. Lett.* **10** 531
- [7] Kobayashi M and Maskawa T 1973 *Prog. Theor. Phys* **49** 652
- [8] Towner I S and Hardy J C 1973 *Nucl. Phys. A* **205** 33
- [9] Hardy J C and Towner I S 2009 *Phys. Rev. C* **79** 055502
- [10] Beringer J *et al.* (Particle Data Group) 2012 *Phys. Rev. D* **86** 010001
- [11] Towner I S and Hardy J C 2010 *Rep. Prog. Phys.* **73** 046301
- [12] Hardy J C and Towner I S 2013 *Ann. Phys.(Berlin)* **525** 443
- [13] Hardy J C and Towner I S 2009 *Nucl. Phys. A* **254** 221
- [14] Hardy J C *et al.* 1990 *Nucl. Phys. A* **509** 429
- [15] Hardy J C and Towner I S 2005 *Phys. Rev. C* **71** 055501
- [16] Eronen T *et al.* 2009 *Phys. Rev. Lett.* **103** 252501

- [17] Eronen T *et al.* 2011 *Phys. Rev. C* **83** 055501
- [18] Eronen T and Hardy J C 2012 *Eur. Phys. J. A* **48** 48
- [19] Freeman J M, Jenkin J G and Murray G 1966 *Phys. Lett.* **22** 177
- [20] Squier G T A, Burcham W E, Hoath S D, Freeman J M, Barker P H and Petty R J 1976 *Phys. Lett.* **65B**, 122
- [21] Barker P H, White R E, Naylor H and Wyatt N S 1977 *Nucl. Phys. A* **279** 199
- [22] Tolich N R, Barker P H, Harty P D and Amundsen P A *Phys. Rev. C* **67** 035503
- [23] Brindhaban S A and Barker P H 1994 *Phys. Rev. C* **49** 2401
- [24] Kikstra S W, Guo Z, Van der Leun C, Endt P M, Raman S, Walkiewicz T A, Starner J W, Journey E T and Towner I S 1991 *Nucl. Phys. A* **529** 39
- [25] Koslowsky V T, Hardy J C, Hagberg E, Azuma R E, Ball G C, Clifford E T H, Davies W G, Schmeing H, Schrewe U J and Sharma K S 1987 *Nucl. Phys. A* **472** 419
- [26] Brown L S and Gabrielse G 1986 *Rev. Mod. Phys.* **58** 233
- [27] Redshaw M, McDaniel J and Myers E G 2008 *Phys. Rev. Lett.* **100** 093002
- [28] Eronen T *et al.* 2006 *Phys. Rev. Lett.* **97** 232501
- [29] Ramsey, N F 1990 *Rev. Mod. Phys.* **62** 541
- [30] Mukherjee M *et al.* 2004 *Phys. Rev. Lett.* **93** 150891
- [31] Savard G *et al.* 2005 *Phys. Rev. Lett.* **95** 102501
- [32] Ringle R *et al.* 2007 *Phys. Rev. C* **75** 055503
- [33] Vonach H, Glaessel P, Huenges E, Maier-Komor P, Roesler H, Scheerer H J, Paul H and Semrad D 1977 *Nucl. Phys. A* **278** 189
- [34] Eronen T *et al.* 2008 *Phys. Rev. Lett.* **100** 132502
- [35] Faestermann T, Hertenberg R, Wirth H-F, Krücken R, Mahgoub, M and Maier-Komor P 2009 *Eur. Phys. J A* **42** 339
- [36] Ryder J S, Clark G J, Draper J E, Freeman J M, Burcham W R and Squier G T A 1973 *Phys. Lett.* **43B** 30
- [37] Azuelos G and Kitching J E 1975 *Phys. Rev. C* **12** 563
- [38] Koslowsky V T, Hagberg E, Hardy J C, Azuma R E, Clifford E T H, Evans H C, Schmeing H, Schrewe U J and Sharma K S 1983 *Nucl. Phys. A* **405** 29
- [39] Finlay P *et al.* 2011 *Phys. Rev. Lett.* **106** 032501
- [40] Park H I, Hardy J C, Iacob V E, Chen L, Goodwin J, Nica N, Simmons E, Trache L and Tribble R E 2012 *Phys. Rev. C* **85** 035501
- [41] *A Handbook of Radioactivity Measurements Procedures* 1985, National Council on Radiation Protection and Measurements, NCRP Report No. 58, Section 3.5
- [42] Park H I *et al.* 2011 *Phys. Rev. C* **84** 065502
- [43] Tribble R E, Burch R H, Gagliardi C A 1989 *Nucl. Instrum. Methods A* **285** 441
- [44] Iacob V E *et al.* 2010 *Phys. Rev. C* **82** 035502
- [45] Chen L, Hardy J C, Bencomo M, Horvat V, Nica N and Park H I 2013 *Nucl. Instrum. Methods A* **728** 81
- [46] Laffoley A T *et al.* 2013 *Phys. Rev. C* **88** 015501
- [47] Grinyer G F *et al.* 2007 *Nucl. Instrum. Methods A* **579** 1006
- [48] Hagberg E, Koslowsky V T, Hardy J C, Towner I S, Hykawy J G, Savard G and Shinozuka T 1994 *Phys. Rev. Lett.* **73** 396
- [49] Finlay P *et al.* 2008 *Phys. Rev. C* **78** 025502
- [50] Hardy J C, Carraz L C, Johnson B and Hansen P G 1977 *Phys. Lett.* **71B** 307
- [51] Hardy J C and Towner I S 2002 *Phys. Rev. Lett.* **88** 252501
- [52] Savard G, Galindo-Uribarri A, Hagberg E, Hardy J C, Koslowsky V T, Radford D C and Towner I S 1995 *Phys. Rev. Lett.* **74** 1521
- [53] Fujikawa B K *et al.* 1999 *Phys. Lett.* **B449** 6
- [54] Sidhu G S and Gerhart J B 1966 *Phys. Rev.* **148** 1024
- [55] Towner I S and Hardy J C 2005 *Phys. Rev. C* **72** 055501

- [56] Park H I *et al.* 2014, to be published
- [57] Helmer R G, Hardy J C, Iacob V E, Sanchez-Vega M, Neilson R G and Nelson J 2003 *Nucl. Instrum. Methods A* **511** 360
- [58] Helmer R G, Nica N, Hardy J C and Iacob V E 2004 *Appl. Rad. Isot.* **60** 173
- [59] Berman S M 1958 *Phys. Rev.* **112** 267
- [60] Kinoshita T and Sirlin A 1959 *Phys. Rev.* **113** 1652
- [61] Sirlin A 1967 *Phys. Rev. Lett.* **19** 877
- [62] Sirlin A 1974 *Nucl. Phys.* **B71** 29
- [63] Sirlin A 1978 *Rev. Mod. Phys.* **50** 573
- [64] Jaus W and Rasche G 1970 *Nucl. Phys.* **A143** 202
- [65] Jaus W 1972 *Phys. Lett.* **40** 616
- [66] Towner I S and Hardy J C 1984 in *Proceedings of the Seventh International Conference on Atomic Masses and Fundamental Constants* ed. Klepper O (Gesellschaft für Schwerionenforschung, Darmstadt) 564
- [67] Sirlin A and Zucchini R 1986 *Phys. Rev. Lett.* **57** 1994
- [68] Sirlin A 1987 *Phys. Rev.* **D35** 3423
- [69] Jaus W and Rasche G 1987 *Phys. Rev.* **D 35** 3420
- [70] Jaus W and Rasche G 1990 *Phys. Rev.* **D 41** 166
- [71] Barker F C, Brown B A, Jaus W and Rasche G 1992 *Nucl. Phys.* **A540** 501
- [72] Towner I S 1992 *Nucl. Phys.* **A540** 478
- [73] Towner I S 1994 *Phys. Lett.* **B333** 13
- [74] Marciano W J and Sirlin A 2006 *Phys. Rev. Lett.* **96** 032002
- [75] Czarnecki A, Marciano W J and Sirlin A 2004 *Phys. Rev.* **D 70** 093006
- [76] Towner I S and Hardy J C 2008 *Phys. Rev.* **C 77** 025501
- [77] Damgaard J 1969 *Nucl. Phys.* **A130** 233
- [78] Towner I S, Hardy J C and Harvey M 1977 *Nucl. Phys.* **A284** 269
- [79] Towner I S and Hardy J C 2002 *Phys. Rev.* **C 66** 035501
- [80] Ormand W E and Brown B A 1985 *Nucl. Phys.* **A440** 274
- [81] Ormand W E and Brown B A 1989 *Phys. Rev. Lett.* **62** 866
- [82] Ormand W E and Brown B A 1995 *Phys. Rev.* **C 52** 2455
- [83] Sagawa H, van Giai N and Suzuki T 1986 *Phys. Rev.* **C 53** 2163
- [84] Liang H, van Giai N and Meng J 2009 *Phys. Rev.* **C 79** 064316
- [85] Auerbach N 2009 *Phys. Rev.* **C 79** 035502
- [86] Miller G A and Schwenk A 2008 *Phys. Rev.* **C 78** 035501
- [87] Miller G A and Schwenk A 2009 *Phys. Rev.* **C 80** 064319
- [88] Grinyer G F, Svensson C E and Brown B A 2010 *Nucl. Instrum. Methods A* **622** 236
- [89] Satula W, Dobaczewski J, Nazarewicz W and Werner T R 2012 *Phys. Rev.* **C 86** 054316
- [90] Moulson M 2012, 11th Conf. on the Intersections of Nuclear and Particle Physics (CIPANP 2012), *AIP Proceedings* **1560**, 117
- [91] Ceccucci A, Ligeti Z and Sakai Y 2012 *The CKM quark-mixing matrix*, a mini-review in [10]
- [92] Blucher E and Marciano W J 2012 V_{ud} , V_{us} , the Cabibbo angle, and CKM unitarity, a mini-review in [10]
- [93] Naviliat-Cuncic O and González-Alonso M 2013 *Ann. Phys.(Berlin)* **525** 600
- [94] Marciano W J 2013, private communication